Appl. Phys. A 73, 199–208 (2001) / Digital Object Identifier (DOI) 10.1007/s003390000686

Applied Physics A
Materials
Science & Processing

Pulsed laser ablation of solids: transition from normal vaporization to phase explosion

N.M. Bulgakova[1], **A.V. Bulgakov**[1,2]

[1] Institute of Thermophysics SB RAS, prosp. Lavrentyev 1, 630090 Novosibirsk, Russia
(Fax: +7-3832/34-3480, E-mail: nbul@itp.nsc.ru)
[2] School of Physics and Engineering Physics, Göteborg University and Chalmers University of Technology, 41296 Göteborg, Sweden
(Fax: +46-31/772-3496, E-mail: bulgakov@fy.chalmers.se)

Received: 18 May 2000/Accepted: 14 July 2000/Published online: 22 November 2000 –

Abstract. We present experimental data on mass removal during 1064-nm pulsed laser ablation of graphite, niobium and $YBa_2Cu_3O_{7-\delta}$ superconductor. Evidence for the transition from normal vaporization to phase explosion has been obtained for these materials, showing a dramatic increase in the ablation rate at the threshold fluences of 22, 15 and 17.5 J/cm^2, respectively. A numerical model is used to evaluate the ablation rate and temperature distribution within the targets under near-threshold ablation conditions. The results are analyzed from the viewpoint of the vaporized matter approaching the critical point with increasing laser fluence. A possible means of the estimating the thermodynamic critical temperature from the data for nanosecond laser ablation is discussed. It is suggested that the critical temperature of refractory metals is higher than that estimated with the traditional methods due to plasma effects. An analogy with the boiling crisis (the transition from nucleate to film boiling) is drawn to explain the formation of ablation craters with spallated edges.

PACS: 79.20.Ds; 64.70.Fx; 64.90.+b

For the last two decades, pulsed laser ablation (PLA) of solids has been subjected to an increasing research interest owing to expanding applications (film deposition, material processing, cluster and nanostructure production, etc.). Despite growing penetration into the processes taking place during PLA, the mechanisms of laser vaporization of materials are still not fully understood. For metals and metal-like materials, three mechanisms are generally referred to when looking at thermal processes: normal vaporization, normal boiling and explosive boiling (phase explosion). For nanosecond laser pulses, the regime of normal vaporization gives way to phase explosion with increasing laser fluence when the irradiated matter approaches the thermodynamic critical point (CP) [1–3].

Martynyuk [4] was the first who proposed that phase explosion of metals irradiated by a laser pulse could be used to determine their critical parameters. On the basis of metal-vaporization experiments on microsecond time scales by both laser pulses and electric explosion of wires, Martynyuk developed an empirical theory that allowed the estimation of the thermodynamic critical temperature, T_c, for a broad spectrum of metals. In spite of possible kinetic limitations [4], there exist a number of experimental evidences that phase explosion is realized at nanosecond time scales [5–8] and even for ps pulses [9, 10]. From the thermodynamic viewpoint, such regimes may be more favorable for studying the critical parameters, since the thermal conductivity plays a minor role and matter can be heated closer to the spinodal. An important contribution to an understanding of the phase-explosion origin has been made by Kelly and Miotello [1–3, 11]. Based on a careful analysis of different heating processes which lead to material removal, they found that explosive boiling is the most efficient mechanism for thermal ablation on short time scales (ns or less). However, the qualitative characterization of the laser-irradiated matter under explosive-boiling regimes still imposes a considerable challenge. An examination of such regimes can help to explain a number of the unclear phenomena observed under pulsed laser ablation and, on the other hand, laser ablation may be a promising technique for the study of critical phenomena in the fast processes.

In this work we carried out experimental and theoretical studies on material-removal mechanisms during PLA with infrared nanosecond pulses under irradiation conditions typically used for thin-film deposition. Based on the measurements of ablation rate as a function of laser fluence, evidence for the transition from normal vaporization to phase explosion has been obtained for a number of materials. Also, time-resolved measurements of the PLA plume transmission have been performed. The experimental data are compared with the results of model calculations based on the conception of normal vaporization. This allowed us to evaluate the temperature distribution within the irradiated target up to fluences when the transition to phase-explosion mechanism occurs. The results are discussed from the viewpoint of the theory of critical phenomena [12, 13]. In this paper, we do not analyze the non-thermal (electronic) processes induced by IR laser radiation in the target, since they play most likely only a minor role under the considered conditions [2, 14].

1 Experimental procedure and the model

The experimental arrangement has been reported in detail elsewhere [15]. In brief, vaporization of the target materials was carried out under vacuum conditions (10^{-3} Pa) with a Q-switched Nd:YAG laser (1064-nm wavelength, pulse of Gaussian profile of 13-ns (FWHM) duration) in the range of laser fluences 1–25 J/cm^2 and irradiation spot size 0.2–1 mm (spot size and pulse energy were varied independently). The experiments were performed with three types of targets: polycrystalline graphite (99.99% purity), pure niobium and $YBa_2Cu_3O_{7-\delta}$ superconductor (YBCO). The targets were irradiated at normal incidence. Mass removal per pulse was determined by measuring the target weight before and after irradiation. The measurements were performed with a translating target to avoid formation of a crater at its surface and the ablation mass was averaged over 500–1000 shots. The temporal dependence of the transmission coefficient of the laser light through the generated plasma plume was measured using a target with a small hole (~ 30 μm) within the irradiated spot using a procedure described in [15].

The theoretical description of laser-induced target heating and material removal was based on the model proposed in [15]. This model, similar in many respects to those developed previously [16–19], takes into account heating of a laser-produced plasma due to absorption of part of the laser energy. This allows one to describe mass removal over a fairly wide range of laser fluences. The details of the model have been described in [15]. Here we repeat only its main features. The time-dependent temperature distribution along the target depth $T(t, z)$ is governed by the heat-flow equation in a one-dimensional form, as appropriate to many experimental situations:

$$c_p\varrho\left(\frac{\partial T}{\partial t}-u(t)\frac{\partial T}{\partial z}\right)=\frac{\partial}{\partial z}\lambda\frac{\partial T}{\partial z} + [1-R(T_s)]\,\alpha_b I(t)\exp(-\alpha_b z)\,. \quad (1)$$

Here ϱ is the mass density of the target material; c_p, λ and α_b are the thermal capacity, the thermal conductivity and the absorption coefficient of the target; $R(T_s)$ is the reflection coefficient considered here to be dependent on the surface temperature T_s; and $u(t)$ is the velocity of surface recession. The $u(t)$ value is defined under the assumption that the flow of vaporized material from the surface follows the Hertz–Knudsen equation and the vapor pressure above the vaporized surface can be estimated with the Clausius–Clapeyron equation:

$$u(t)=0.82\frac{p_b}{\varrho}\left(\frac{m}{2\pi kT_s}\right)^{1/2}\exp\left[\frac{L}{k}\left(\frac{1}{T_b}-\frac{1}{T_s}\right)\right]\,, \quad (2)$$

where L is the latent heat of the target material, k is the Boltzmann constant, and T_b is the boiling temperature under the reference pressure p_b. The parameters p_b and T_b are taken only as normalizing values and do not assume the boiling vaporization mechanism. The intensity of laser light reaching the target surface is written as follows:

$$I(t)=I_0(t)\exp[-\Lambda(t)] = I_0(t)\exp\left[-\int_0^\infty \alpha(n_p, T_p)\mathrm{d}z\right]\,, \quad (3)$$

where $I_0(t)$ is the incident laser intensity, $\Lambda(t)$ is the total optical thickness of the PLA plasma and $\alpha(n_p, T_p)$ is the plasma absorption coefficient dependent on the plasma density and temperature. The initial and boundary conditions are

$$T(0,z)=T_0,\quad T(t,0)=T_s(t),\quad \lambda\left.\frac{\partial T}{\partial z}\right|_{z=0}=Lu(t) \quad (4)$$

with T_0 being the initial temperature uniform across the target.

For a low-temperature equilibrium plasma, the absorption coefficient can be written as $\alpha = n f(T)$, where $f(T)$ is an increasing function of the temperature [20]. The increase of the plasma temperature due to radiation absorption can be estimated as $\Delta T=(\gamma-1)E_a/kN=(\gamma-1)mE_a/(k\Delta z\varrho)$, where $\Delta z(t)$ is the ablation depth, $E_a(t)$ is the density of the laser energy absorbed by the plasma, γ is the specific heat ratio and N is the total number of the vaporized particles. After a series expansion of $\alpha(t)$ in terms of ΔT and restriction to the linear term we obtain

$$\Lambda(t)=a\Delta z(t)+bE_a(t)\,. \quad (5)$$

Here, a and b are the time-independent coefficients:

$$a=\varrho f(T_v)/m,\quad b=\frac{(\gamma-1)}{k}\left.\frac{\partial f}{\partial T}\right|_{T_v}\,, \quad (6)$$

where T_v is the temperature at which the particles are vaporized. Strictly speaking, T_v is not fixed for normal vaporization. However, the approximation of constant values for a and b is reasonable for ns laser pulses of moderate intensity when the main vaporization occurs in a time interval during which T_v changes little, not exceeding $(0.85-0.9)T_c$ [2, 4, 19]. The coefficients a and b, being the only free parameters in the model, were determined by fitting the experimental and calculated data on mass removal. The model was found to describe accurately the dynamics of IR radiation absorption by the PLA plume [15]. The parameters used for calculations and the obtained adjustable coefficients are summarized in Table 1. In the table we have accumulated the data on the temperature dependences of the thermal and optical parameters available to date.

2 Results and discussion

2.1 Mass removal and surface temperature

The experimental and calculated data on mass removal as functions of the laser fluence for graphite, YBCO and Nb are shown in Fig. 1. The results derived from modeling using (1)–(6) are given by solid curves. The calculated data match well the experimental points up to a threshold value of laser fluence (referred to below as 'threshold fluence'), following which a sudden increase of mass removal occurs. This jump in ablation rate is accompanied by the appearance of considerable amounts of droplets in the plume, which indicates a transition to a different vaporization regime. Above the threshold fluence, an essential fraction of the vaporized materials is emitted as micrometer-size particulates which are visible to the unaided eye as

Table 1. The properties of graphite, YBCO superconductor and niobium used for model calculations

Graphite	
Atomic mass	12 u
Density (20 C)[a]	1.87 g/cm^3
Boiling temperature (at 10^5 Pa)[b,c]	4473 C
Latent heat[c,d]	718.87 kJ/mol
Absorption coefficient[e]	1.5×10^5 cm^{-1}
Reflection coefficient[f,g]	$0.21 - 2.83 \times 10^{-5}(T - 300),\ T \le 7000$ K
	$0.02,\ T > 7000$ K
Specific heat, J/(kg K)[b,g]	$1727 + 0.333T - 3.106 \times 10^5/T,\ T \le 1500$ K
	$2019.4,\ T > 1500$ K
Thermal conductivity, W/(m K)[g,h]	$6 \times 10^4/T,\ T \le 3000$ K
	$20,\ T > 3000$ K
Adjustable parameters characterizing plasma absorption	$a = 2500$ cm^{-1}
	$b = 0.57$ cm^2/J
YBCO	
Average mass of vaporized species[i]	89 u
Density (20 C)[a]	4.55 g/cm^3
Sublimation temperature (at 10^5 Pa)[j]	2173 K
Latent heat[k]	430.3 kJ/mol
Absorption coefficient[l]	5×10^4 cm^{-1}
Reflection coefficient[l,m]	0.15
Specific heat, J/(kg K)[n,g]	$325 + 0.25T,\ T \le 700$ K
	$2210 + 1.56T - 1.72 \times 10^{-3}T^2 - 1.37 \times 10^6/T,\ 700\text{ K} < T \le 1100$ K
	$600,\ T > 1100$ K
Thermal conductivity, W/(m K)[o,g]	3.2
Adjustable parameters characterizing plasma absorption	$a = 27\,000$ cm^{-1}
	$b = 0.43$ cm^2/J
Niobium	
Atomic mass	93 u
Density (20 C)[b]	8.57 g/cm^3
Boiling temperature (at 10^5 Pa)[b]	5073 K
Latent heat[c,d]	722.8 kJ/mol
Absorption coefficient[e]	5×10^5 cm^{-1}
Reflection coefficient[e,p,g]	$0.75 - 6.12 \times 10^{-5}(T - 300),\ T \le 2750$ K
	$0.6 - 8 \times 10^{-4}(T - 2750),\ 2750\text{ K} < T \le 3000$ K
	$0.4 - 5.7142 \times 10^{-5}(T - 300),\ 3000\text{ K} < T \le 6500$ K
	$0.2,\ T > 6500$ K
Specific heat, J/(kg K)[q]	$284.65 - 4.387 \times 10^{-3}T - 2.01 \times 10^6/T^{-2} + 2.26 \times 10^{-5}T^2,\ T \le 2750$ K
	$443.18,\ T > 2750$ K
Thermal conductivity, W/(m K)[b,g]	$49 + 0.015T,\ T \le 1067$ K
	$65,\ T > 1067$ K
Adjustable parameters characterizing plasma absorption	$a = 60\,000$ cm^{-1}
	$b = 0.937$ cm^2/J

[a] Measured

[b] I.S. Grigoryev, E.Z. Meilikhov, A.A. Radzig (Eds.): *Handbook of Physical Quantities* (CRC Press, 1995)

[c] G.V. Samsonov (Ed.): *Physicochemical Properties of the Elements* (Naukova Dumka, Kiev 1965) (in Russian)

[d] The heat of melting is taken into account

[e] V.M. Zolotarev, V.N. Morozov, E.V. Smirnova: *Optical Constants for Natural and Technical Media* (Khimiya, Leningrad 1984) (in Russian)

[f] N.G. Basov, V.A. Boiko, O.N. Krokhin, O.G. Semenov, G.V. Sklizkov: Sov. Phys. Tech. Phys. **13**, 1581 (1969); A.M. Malvezzi, N. Bloembergen, C.Y. Huang: Phys. Rev. Lett. **57**, 146 (1986)

[g] The expressions have been derived here to approximate the data from the references

[h] A.S. Okhotin (Ed.): *Handbook of Thermal Conductivity of Solids* (Energoatomizdat, Moscow 1984) (in Russian)

[i] R.K. Singh, J. Narayan: Phys. Rev. B **41**, 8843 (1990); A.V. Bulgakov, N.M. Bulgakova: J. Phys. D: Appl. Phys. **28**, 1710 (1995); emission of molecules and clusters is taken into account

[j] R.K. Singh, J. Viatella: J. Appl. Phys. **75**, 1204 (1994)

[k] The value has been estimated (as the energy required to completely dissociate YBCO material into related ablated species) from latent heats of fusion and vaporization of respective oxides (see L. Lynds, B.R. Weinberger, D.M. Potrepka, G.G. Peterson, M.P. Lindsay: Physica C **159**, 61 (1989); D. Battacharya, R.K. Singh, P.H. Holloway: J. Appl. Phys. **70**, 5433 (1991))

[l] A. Bjørneklett, A. Borg, O. Hunderi: Physica A **157**, 164 (1989)

[m] D.E. Aspnes, M.K. Kelly: IEEE J. Quantum Electron. **25**, 2378 (1989)

[n] J. Heremans, D.T. Morelli, G.W. Smith, S.C. Strite III: Phys. Rev. B **37**, 1604 (1988); V.E. Lusternik, V.E. Peletskii, V.S. Bakunov, A.V. Bolotnikov: Superconductivity (USA) **3**, 2037 (1990)

[o] Yu.A. Kirichenko, K.V. Rusanov, E.G. Turina: Superconductivity (USA) **3**, 1385 (1990)

[p] S.I. Anisimov, Ya.A. Imas, G.S. Romanov, Yu.V. Khodyko: *The Effects of High-Power Radiation on Metals* (Nauka, Moscow 1970) (in Russian)

[q] L.V. Gurvich, I.B. Veits, V.A. Medvedev, G.A. Khachkuruzov, V.S. Yungman, G.A. Baibuz, V.S. Iorish, G.N. Yurkov, S.I. Gorbov, I.I. Nazarenko, O.V. Dorofeeva, L.F. Kuratova, E.L. Osina, A.V. Gusarov, V.Ya. Leonidov, I.N. Przhevalsky, A.L. Rogatsky, Yu.M. Efremov, V.G. Ryabova, V.Yu. Zitserman, Yu.G. Khait, E.A. Shenyavskaya, M.E. Efimov, V.A. Kulemza, Yu.S. Khodeev, S.E. Tomberg, V.N. Vdovin, A.Ya. Yakobson, M.S. Demidova (Eds.): *Thermodynamic Properties of Individual Substances. Reference Book* (Nauka, Moscow 1974) Vol. 2, Part 1, p. 72 (in Russian)

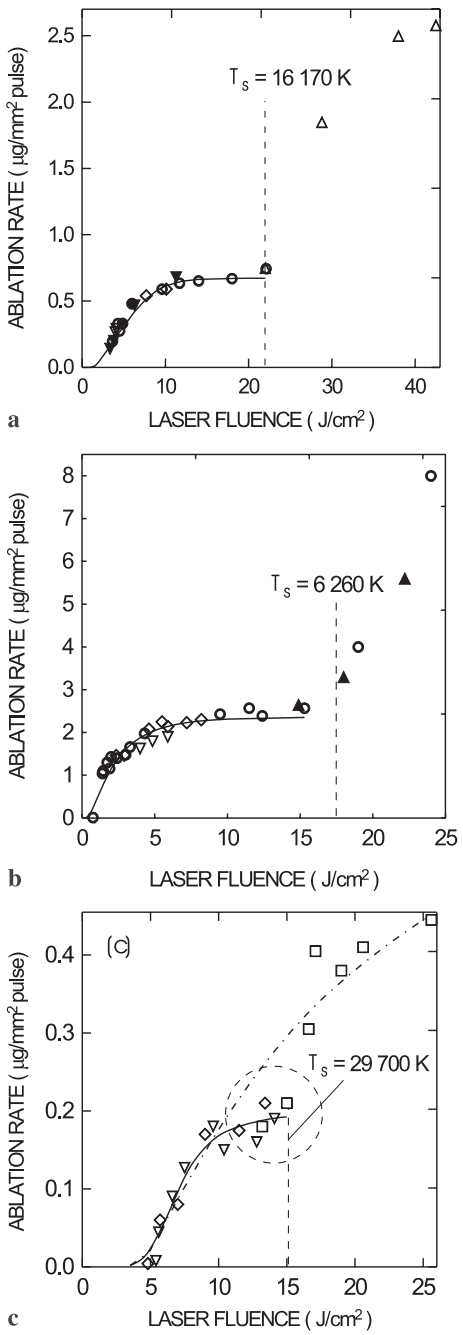

Fig. 1a–c. Mass removal per pulse as a function of laser fluence for the graphite (**a**), YBaCuO superconductor (**b**) and niobium (**c**) targets. Experimental points have been obtained with different spot diameters: Δ – 0.2 mm, $\blacktriangle$ – 0.3 mm, $\square$ – 0.4 mm, $\bigcirc$ – 0.5 mm, $\Diamond$ – 0.6 mm, $\blacktriangledown$ – 0.7 mm, ∇ – 0.8 mm, $\bullet$ – 1 mm. The theoretical results are presented as *solid curves*. The threshold values of laser fluence are indicated by *vertical dashed lines* with the corresponding surface temperatures marked. The preliminary results of modeling for niobium are shown by the *dashed–dotted line*

bright sparks and present in abundance in a deposit when a substrate is introduced into the plume. At sub-threshold fluences, small droplets can also be observed at the substrate, but their amount is fairly small. The threshold laser fluences are found to be 22, 17.5 and 15 J/cm^2 for graphite, YBCO and niobium respectively, as shown by the dashed lines in Fig. 1. The calculated values of the maximum surface temperatures T_s for these fluences are also indicated.

It should be emphasized that, for the materials with small mass removal per pulse like Nb, the mentioned transition is not prominent and can be overlooked. In Fig. 1c, our preliminary fit of the experimental data is shown by a dashed–dotted line. It seemed to be possible to describe the experimental results with only one adjustable parameter $a = 5.5 \times 10^5$ cm^{-1} that indicated almost no heating effect due to plasma absorption [15]. This fact and the appearance of the bright sparks in the plume with increasing laser fluence made us perform an additional check of the data. The points enclosed in the dashed circle are the result of this check that shows a change of the vaporization regime for Nb similar to that observed for the graphite and YBCO targets. The adjustable parameters a and b resulting from the final fit (solid line in Fig. 1c) are given in Table 1.

We attribute the observed change of the vaporization regime to the initiation of the phase explosion which develops as the surface temperature rises up to $\sim 0.9T_c$ [2–4]. Note that the recently observed similar behavior (drastic increase in ablation rate, threshold-like ejection of large droplets) during excimer PLA of nickel specimens was also discussed in terms of explosive-type vaporization [6]. It is of interest to analyze the behavior of the target temperature from the viewpoint of approaching the thermodynamic critical temperature. The calculated values of maximum surface temperature are given in Fig. 2 as a function of laser fluence for the studied materials. In a qualitative sense, these dependences for graphite and YBCO targets are very similar to the corresponding ones of mass removal (see Fig. 1): a fast increase at low fluences is followed by a saturation with increasing fluence. For the niobium target, however, the maximum T_s value increases more steeply up to the laser fluence where phase explosion takes place. This implies a different character of approaching T_c for this material. Based on the obtained experimental and calculated results for different targets, below we analyze a number of thermal heating processes which play, in our view, a role under near-transition PLA conditions.

One may argue that the calculated values of the surface temperature are too high at the near-transition regimes, while the model implies the temperature dependences of the

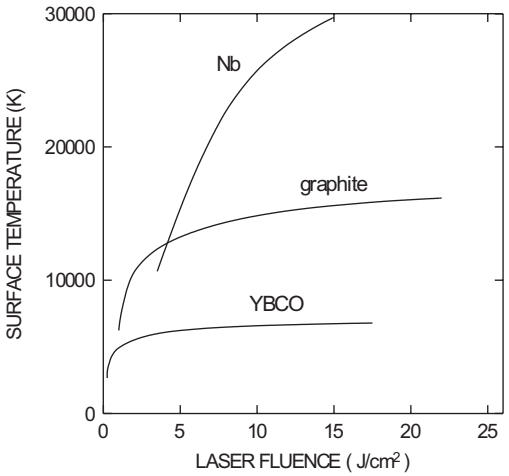

Fig. 2. The calculated maximum surface temperature of graphite, Nb and YBCO targets as a function of laser fluence

thermal and optical parameters only for relatively low temperatures (Table 1). The calculations have shown that, if one assumes normal vaporization (that is, the recession velocity is defined by (2)), the experimental value of mass removal can be described only with a certain surface temperature, high enough for the near-threshold fluences. Any attempts to restrict the surface temperature, taking into account power-law dependences for the thermal parameters inherent in the neighborhood of the CP (increasing thermal conductivity and specific heat and decreasing latent heat with increasing temperature) [12, 13], resulted in a strong decrease of the mass removal, which is inconsistent with the experimental data. As the behavior of the thermal and optical parameters of specific substances at high temperatures is still an open question (according to the dynamic scaling theory [13] the parameters have no time to relax to their equilibrium values at such fast processes like ns laser ablation), we will restrict our discussion to the results obtained with the values cited in Table 1. An argument in favor of the correctness of the model at fairly high temperatures is that such an approach allows us to describe the plasma absorption effect over a wide fluence range without any additional adjustable parameters [15].

2.2 Plasma absorption

Saturation of the ablation rate with fluence is the result of screening of the target surface by the PLA plasma plume. The role of plasma screening in surface-temperature behavior is illustrated in Fig. 3. The calculated time dependences of the surface temperature are given in Fig. 3a for the graphite target irradiated with different laser fluences. Figure 3b illustrates the effect of plasma absorption on the temporal profile of laser radiation that penetrates to the target surface through the PLA plume. At low laser fluences (curve for $1.75\,\mathrm{J/cm^2}$, Fig. 3a) the surface temperature continues to rise after reaching the laser-radiation maximum. This means that the maximum vaporization rate is delayed relative to the laser pulse. As the laser fluence increases with a corresponding increase of mass removal, T_s is peaked at earlier times with respect to the incident laser-pulse maximum as the result of plasma absorption (see curves for $18\,\mathrm{J/cm^2}$ in Fig. 3a,b). Both experimental and calculated results obtained show that, despite rather small mass removal, the niobium plasma plume absorbs somewhat more as compared to the carbon plume (Fig. 3b). Strong absorption of laser radiation in the niobium plasma plume is most likely the result of a high ionization degree of the plume particles due to the relatively low ionization potential. Therefore, the difference noted above in the surface-temperature behavior (Fig. 2) is not associated with plasma plume absorption and should be presumably searched for in the thermal properties of the vaporized solids.

2.3 Subsurface heating

Subsurface heating has been shown to occur under certain conditions during irradiation of solid targets by laser pulses of microsecond duration [21–23]. For nanosecond pulses this effect has been found to be of minor importance for metal targets [1, 11]. Our calculations reveal significant subsurface

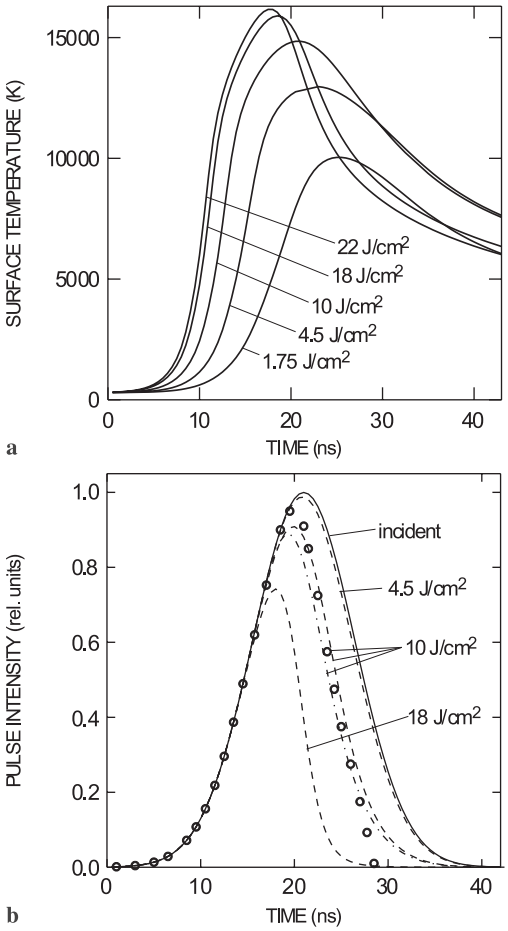

Fig. 3. a The calculated time dependences of the surface temperature for the graphite target at certain laser fluences. **b** Calculated temporal profiles of laser radiation penetrating to the target surface through the PLA plasma at certain laser fluences during graphite (*dashed curves*) and Nb (*dot–dashed curve*) ablation. The incident laser pulse, peaked in the calculations at 20.5 ns, is shown by a *solid curve*. The *points* represent the experimental data for graphite at $10\,\mathrm{J/cm^2}$

heating for non-metal targets. Figure 4 shows the spatial behavior of the calculated target temperature for three studied materials (distributions into the bulk along the normal to the target surface). The distributions for both low laser fluences (Fig. 4a) and high fluences (corresponding to the transition to phase explosion, Fig. 4b) are given for the time moments when the surface temperature T_s reaches its maximum value. These moments differ for different materials and fluences (see Fig. 3a). From Fig. 4a,b it is obvious that again the Nb target behaves distinctively. The values of subsurface heating in this case, $\Delta T = T_{max} - T_s$ (T_{max} being the maximum temperature in spatial distribution) are negligibly small compared with T_s values ($\sim 2\,\mathrm{K}$ at $5\,\mathrm{J/cm^2}$ and $\sim 22\,\mathrm{K}$ at $15\,\mathrm{J/cm^2}$). For graphite and YBCO, subsurface heating is noticeable even at low fluences and reaches thousands of kelvin at threshold fluences (maximum subsurface temperature is 22 400 and 11 600 K, respectively). The depth of maximum subsurface heating is about 50 nm, which is ~ 230 monolayers for graphite. Almost no subsurface heating ($\Delta T \sim 2\,\mathrm{K}$) was previously obtained for aluminum at $4\,\mathrm{J/cm^2}$ [1]. It is important to understand whether or not subsurface heating is a common feature of PLA and what its value depends on, especially in view

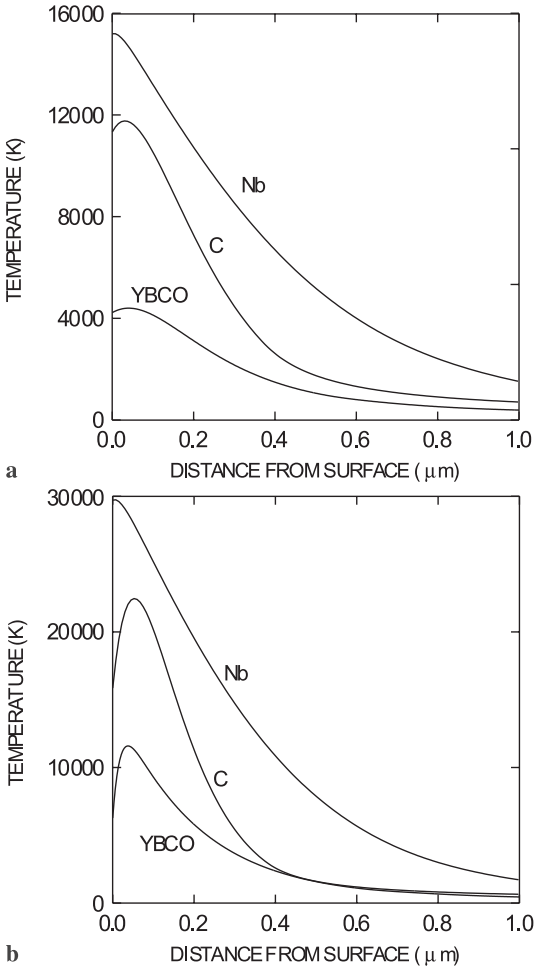

Fig. 4a,b. The calculated temperature profiles within the targets at the time moments when the surface temperature reaches its maximum value. **a** Distributions obtained for low laser fluences (2.5, 0.5 and 5 J/cm^2 for graphite, YBCO and Nb, respectively). **b** Distributions obtained for the fluences corresponding to thresholds from normal vaporization to phase explosion (22, 17.5 and 15 J/cm^2 for graphite, YBCO and Nb, respectively)

of the fact that the model of subsurface heating has been criticized on the basis of its 'probable non-existence' or negligible value [1–3, 11].

During the laser pulse, the temperature spatial distribution in the bulk is formed as the result of the superposition of (i) heating due to laser-energy absorption, (ii) cooling of the target surface due to vaporization and (iii) cooling due to thermal conductivity. Consider in more detail the effects of these factors for different materials.

(i) Absorption of the laser energy is a volume process governed by the Beer–Lambert law (last term in (1)). The smaller the absorption coefficient α_b, to a greater depth the laser energy penetrates the target. Among the materials studied, niobium has the greatest α_b (Table 1), that is the laser energy is absorbed in a thinner layer near the target surface, resulting in a higher temperature rise, as compared to graphite and YBCO.

(ii) An important feature of the models based on the concept of *normal vaporization* is that surface cooling due to the heat of vaporization is taken into account through the boundary condition (4), which defines the temperature gradient at the surface $(\partial T/\partial z)\,|_{z=0}$ from the recession velocity [1, 17]. The latter is determined by the surface temperature through the Clausius–Clapeyron equation (2). It may be concluded that the higher the recession velocity, the more possible is subsurface heating. Turning back to Fig. 1, we see that niobium has the smallest mass removal, which is the result of the smallest recession velocity. Thus, the niobium surface is cooled due to the heat of vaporization to a lesser extent as compared to graphite and YBCO.

(iii) The rate of temperature equalization along the distance with time is controlled by the temperature conductivity $\chi = \lambda/(\varrho c_p)$, as clearly follows from the simplest form of the heat-diffusion equation assuming temperature-independent material parameters:

$$\frac{\partial T}{\partial t} = \frac{\lambda}{\varrho c_p}\frac{\partial^2 T}{\partial z^2}\,. \tag{7}$$

For fairly high temperature, when the parameters adopted in the present calculations are constant (Table 1), the χ values for graphite, YBCO and Nb are 0.053, 0.011 and 0.17 cm^2/s, respectively. Thus, subsurface heating of the Nb target, if it occurs, flattens more quickly as compared to graphite and YBCO. Note that in the niobium target the heat is conducted to the bulk depth faster as well (Fig. 4).

The listed factors (i)–(iii) result therefore in a common tendency for the Nb target to have the least chance for subsurface heating among the materials studied. Note that aluminum appears to have even less probability to exhibit the subsurface-heating effect during PLA since its temperature conductivity (0.89 and 0.40 cm^2/s for solid and liquid states, respectively [16]) is considerably higher than that of Nb. Based on the negligible value of the calculated temperature difference $T_{max} - T_s$ found for the Al target, it was claimed that subsurface heating has a very minor effect under normal vaporization conditions [11, 16]. We argue that this statement, being correct for metals, is not true for materials like graphite and YBCO.

Anisimov et al. [24] introduced a parameter $\beta = \alpha_b \chi/u$ to characterize the ablation regime for millisecond laser pulses when quasi-stationary vaporization is realized. This parameter combines the factors listed in items (i)–(iii) and accounts for the ratio of target-heating rate to the recession velocity. If $\beta > 1$, an approach based on the concept of *normal vaporization* is valid and the subsurface-heating effect can be evaluated as $\Delta T \approx L/(c_p\beta)$ [21–23]. If $\beta < 1$, then $\Delta T \approx L/c_p \sim T_c$ and *phase explosion* of the metastable matter occurs [21, 22]. We used such an approach to estimate subsurface heating for the regimes studied. For the estimations, the average value of the calculated recession velocity $\Delta z/\tau$ (with Δz taken at *threshold fluence*) was used. The results are summarized in Table 2. The estimation and available data for Al are also included. There is surprisingly good agreement between the estimated and calculated ΔT values. This simple method can therefore provide a reasonable evaluation of the subsurface-heating effect during PLAs: However, the β-criterion for *transition* to phase explosion obviously fails for ns laser pulses since the β values under transition conditions differ dramatically for the materials studied and for Nb and Al they far exceed unity. This indicates that the behavior of condensed matter in the vicinity of the transition ablation regime is different for ms and ns pulses. In the lat-

Table 2. Estimated subsurface heating and the relevant data

Parameter	Graphite	YBCO	Niobium	Aluminum[a]
Temperature conductivity χ, cm^2/s	0.053	0.011	0.17	0.89
L/c_p, K	2.96×10^4	8.06×10^3	1.607×10^4	1.12×10^4
Δz, cm	0.35×10^{-4}	0.55×10^{-4}	2×10^{-6}	7×10^{-6} [b]
$\beta = \alpha_b \chi \tau / \Delta z$	2.95	0.13	552.5	2543
$\Delta T = T_{max} - T_s \approx L/(c_p \beta)$, K	$\sim 10^4$	$\sim 8 \times 10^3$ [c]	~ 29	~ 5
$\Delta T = T_{max} - T_s$, K, calculated	6.23×10^3 [d]	5.34×10^3 [d]	22 [d]	~ 2 [e]

[a] Parameters for Al have been taken from [16]
[b] A.J. Pedraza, J.-Y. Zhang, H. Esrom: Mater. Res. Soc. Symp. Proc. **285**, 209 (1995). This value has been taken for $\lambda = 351$ nm, laser fluence of $3.8\,J/cm^2$ and 40-ns pulse duration
[c] For $\beta < 1$, $T_{max} - T_s \approx L/c_p$ [21]
[d] Present calculations
[e] Calculated in [1] for $4\,J/cm^2$

ter case, the heating rate is higher and the substance can be therefore heated closer to T_c.

We should note that the model used in this work is quite simple and thus the fairly high values of subsurface heating obtained in the calculations are possibly not entirely realistic. What we want to emphasize here is that the subsurface-heating effect cannot be neglected for a number of materials under certain PLA conditions with *normal vaporization* of the irradiated target, as has been demonstrated by solving the heat-diffusion equation with a *non-fixed* surface temperature. In particular, for graphite considerable subsurface heating has been obtained even for low fluences (e.g., ~ 400 K at $2.5\,J/cm^2$, see Fig. 4a). The above thermodynamic analysis shows that the subsurface-heating effect depends on a competition between volume heating due to penetration of laser energy into a target, surface cooling due to vaporization and heat conduction into the target bulk. Simple estimations of a balance of these processes argue for the existence of subsurface heating for non-metal targets. We finally note that our model obviously loses its applicability at certain subthreshold fluences when the calculated temperature in the subsurface region approaches T_c.

2.4 Phase explosion and critical phenomena

A typical $p-T$ phase diagram of a substance in the neighborhood of the CP is shown in Fig. 5. The line of equilibrium for the system 'liquid–vapor' (the binodal) originates at the triple point A (a point of coexistence of solid, liquid and vapor) and ends at the CP. To provide a clearer insight into the mechanisms of phase explosion and its possible manifestations, we recall here the basic tenets of the theories of metastable liquids and critical state of matter [12, 13].

(1) As the CP is approached, the fluctuations of the matter parameters are increasing. The density and the entropy thereof undergo the greatest fluctuations as compared to the other parameters (p, T). The matter takes on a fine-grained structure, scattering light (the opalescence phenomenon). Simplifying the picture, one may say that the critical state is 'a gas of droplets' [13] whose characteristic size r_c (or a correlation length) increases when approaching the CP.

(2) If the liquid, being heated, has enough time to relax to a definite equilibrium state (far from the CP, the relaxation time is normally 1–10 ns [12]), the matter is stable and its state follows the binodal. In other words, if the system is heated through the sequence of the equilibrium states, one may use the theory of equilibrium thermodynamics and the Clausius–Clapeyron equation is still valid. However, with increase of the correlation length, the fluctuation theory should be used instead of the classical approach.

(3) The rapidly heated system may undergo superheating. In other words, the temperature of the liquid becomes higher than that of boiling under the given pressure. If so, the system shifts from the binodal into the region I of the metastable states (Fig. 5) and, as the heating rate increases, approaches the spinodal. This leads to a decrease of the lifetime of the system and to an uncertainty of its thermodynamic parameters near the spinodal. The system seeks for equilibrium that results in its return to the binodal through *explosive boiling* (sharp increase of homogeneous nucleation).

(4) The rate of homogeneous nucleation increases dramatically with superheating. The average time for formation of the critical vapor nucleus (a vapor sphere that will grow rather than decay) can drop by 3–4 orders of magnitude with superheating by 1 C, which is conditioned by a fast decrease of both the critical nucleus size and the free energy for formation of a stable nucleus. At the same time, the rate of the vapor-sphere growth increases drastically. The increasing nucleation prevents the liquid from approaching the spinodal, resulting

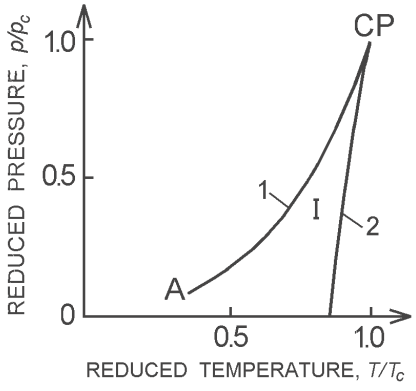

Fig. 5. Typical 'liquid–vapor' phase diagram: 1 is the binodal; 2 is the spinodal; A is the triple point, CP is the critical point. The region I between binodal and spinodal corresponds to the metastable states of matter

in decay of the highly superheated liquid into a mixture of gas and droplets (*phase explosion* or *explosive boiling*). It may be said that the liquid 'is torn into droplets' by growing the numerous gas bubbles.

(5) One of the possible mechanisms for formation of a new phase is the rise of the density gradients inside a small volume of superheated liquid (density fluctuations) that leads to the loss of stability and to the appearance of a vapor bubble. If the metastable region is close to the CP ($T \geq 0.9T_c$), the density gradient necessary for the nucleation due to fluctuations decreases. That is why the closer matter approaches the CP, the more possible is superheating and phase explosion.

(6) For given superheating, the critical nucleus size is much greater for metals than for organic liquids and water. As a result, spontaneous nucleation in liquid metals is not obtained even for large superheating. On fast heating, the metals can thus be heated very close to the critical temperature and only then does phase explosion occur.

(7) Metals lose their metallic properties near the CP. Particularly, the electric conductivity drops because of the disruption of the conductivity zone due to increasing density fluctuations.

A variety of methods were proposed to estimate the thermodynamic critical temperature of materials. Most of them are based on the relation between the critical and boiling temperatures, which was first revealed by Guldberg for a number of substances [25]. The literature on the estimations of T_c is reviewed in [26] where different modifications of the Guldberg law and some other methods are given. All of them are of limited usefulness since they have been developed for limited groups of substances (mostly for organic liquids). A generalization of the Guldberg law for inorganic liquids was proposed in [27] as $T_c = T_b/\theta$, where θ is determined by the vaporization entropy, ΔS_v, as $\theta = a + b/\Delta S_v$ with the coefficients a and b depending on the polarity of the substance molecules. Normally, the θ value is in the range $0.45 - 0.55$ for ionic compounds and $0.25 - 0.5$ for metals. For metal liquids, Martynyuk [4] proposed an empirical equation for the estimation of T_c using the latent-heat value: $T_c = c + dL$ where $c = 860$ K and $d = 15.05 \times 10^{-6}$ kmol K/J.

For refractory metals, however, whose critical temperature is presumably comparable to the ionization potential (see discussion below), all the mentioned methods appear to fail, as was already pointed out in [28]. The reason resides in the fact that under high temperature such a metal may represent a metal plasma. As such a substance is ionized substantially when approaching the CP, it does not lose the electric conductivity. This can influence significantly the interaction between atoms. (Recall that the CP is, in essence, the state of a substance wherein the potential energy of mutual attraction of the molecules is equalized to some extent by their average kinetic energy [26].) One may speculate that free electrons, due to high mobility, tend to escape from the regions of high density to those with low density (as takes place in a plasma), thus breaking down quasi-neutrality. Figure 6 illustrates schematically such an ionized state of a metal. Therefore, in addition to the fluctuations in density, temperature, pressure and entropy near the CP, refractory metals may also experience charge fluctuations. The ambipolar electric field, developing in such an ionized substance, should cause the density fluctuations to decrease, thus 'cementing' the substance and increasing the critical temperature. Likalter [29], reasoning about the properties of a metal plasma near the CP, proposed the dependence $T_c \approx 0.085 z^2 I/(z+1)$, where I is the ionization potential and z is the valence.

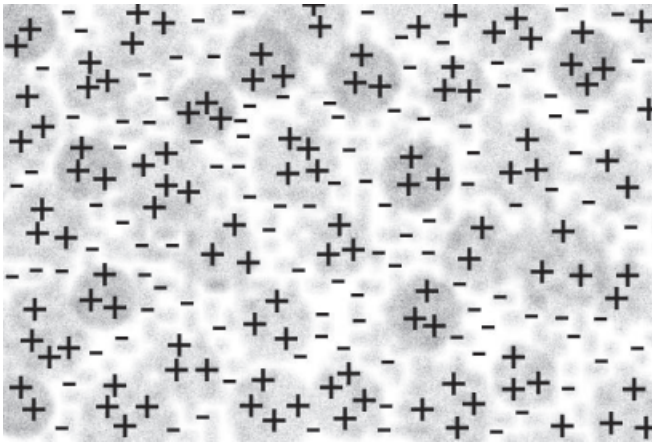

Fig. 6. Sketch representation of a refractory metal near its critical point. The *dark* and *light* areas are the regions with the high and the low density respectively. Free electrons tend to escape from the regions of the high density to those with the low density, causing charge fluctuations

The results on application of the listed methods and the data on the critical temperature from the literature for the materials studied are summarized in Table 3. One can see that the deviations between data may exceed 100%. An attempt to apply Likalter's dependence to niobium has not been successful because of the low valence of Nb atoms (the electron configuration is $4d^4 5s$). However, it is highly probable that the valence changes near the critical point, as in the case of cop-

Table 3. Values of the critical temperature estimated with different methods and/or taken from the literature

Method and references	Graphite	YBCO	Niobium
Guldberg law, $T_c = T_b/\theta$, $\theta = 2/3$ [25]	6710 K	3260 K	7610 K
Generalized Guldberg law [27]	8946–17 892 K [a]	3950–4830 K [b]	10 146–20 292 K
$T_c = c + dL$, $c = 860$ K, $d = 15.05 \times 10^{-6}$ kmol K/J [4]	11 670 K	7330 K	11 730 K
Principle of corresponding states [28]	–	–	19 040 K
Present calculations	22 400 K	11 600 K	29 700 K

[a] The range of θ is taken as for a metal
[b] The range of θ is taken as for an ionic compound

per [29]. Whether the electrons from the inner d-shell, which exhibit valence in various chemical compounds of niobium, may be considered as valent in Likalter's formula remains a question.

Estimations with the Saha equation show that the equilibrium ionization degree of Nb, assuming the density of a liquid, exceeds 1% at $T = 1$ eV, and increases rapidly with further temperature increase ($\sim 4.5\%$ at $T = 1.5$ eV). As the estimated values of the critical temperature are of ~ 1 eV and higher (see Table 3), niobium may not lose the electric conductivity near the CP, as it appears to be substantially ionized. As discussed above, this results in a change of the interaction between the atoms and in an increase of the critical temperature. One would expect that at least several more metals should also exhibit plasma properties in the neighborhood of T_c (e.g., Ti, Y, Zr, Mo, Tc, Hf, Ta, W, Re, Os, Th) due to their relatively low ionization potential and high boiling temperature under normal pressure.

Note that a substantial part of the laser energy coupled to a target should be used for ionization of the mentioned materials at fairly high fluence. A proper correction should therefore be done for a more correct description of the target-temperature behavior under PLA conditions near the transition to phase explosion. Obviously, the subject discussed here invites further investigations.

2.5 Boiling crisis

As mentioned above, a small amount of droplets was observed even for low laser fluence when the ablation rate is well described with the model based on the concept of normal vaporization. The possible physical reason for melt ejection in such a regime is the recoil pressure of the vaporizing material which acts on the molten bottom of the ablation spot, splashing material in the radial direction [30]. With increasing laser fluence, a transition from normal vaporization to phase explosion occurs, so that molten material breaks down into vapor and droplets as a result of explosive boiling. One more inherent phenomenon of boiling, the *boiling crisis*, which may reveal itself during laser ablation, should be considered.

Boiling begins when the liquid bulk temperature slightly exceeds the saturation (boiling) temperature under the pressure of non-vapor ambient above the liquid surface (e.g., due to thermal flux supplied to the liquid from a heated plate placed in the depth of the liquid) [31, 32]. The vapor bubbles are therewith produced at the plate, first in the centers of nucleation (bubbles of gas, microvalleys, etc.), then ascending to the surface (*nucleate* or *normal boiling*). It was shown however that *normal boiling* is subject to major obstacles during both bubble formation and diffusion stages, and hence this ablation mechanism is not important for laser pulses shorter than ~ 100 ns [3, 32]. If liquid is considerably superheated throughout as compared to the saturation temperature (e.g., on a sudden pressure release), bubbles of vapor are produced over all the liquid volume, which is *explosive boiling* or *phase explosion*. On large heat flux supplied to the liquid through the heating plate, boiling transforms from the nucleate regime to the film one. The transformation is a threshold process and is called the *boiling crisis* [31]. A fundamental peculiarity of *film boiling* lies in the fact that the near-plate layer of liquid is heated to the temperature of intense nucleation, so that the bubbles coalesce together and liquid is separated from the heating plate by a vapor layer, resulting in much lower heat-transfer rates compared to nucleate boiling.

A sort of boiling crisis, which may develop under PLA conditions, is presented schematically in Fig. 7. It was already noted that the rate of homogeneous nucleation increases dramatically with minor superheating. The value of superheating in the subsurface target regions, ΔT, depends on the properties of a substance and may be significant under laser ablation conditions (see Table 2). Thus, in the depth of the target, where the temperature maximum is reached, the nucleation frequency is higher than that closer to the surface (Fig. 7a). Under some value of superheating the bubbles can coalesce into a large vapor volume (Fig. 7b), which is inflated due to continuing vaporization from its surface and the pressure gradient across the thin liquid film separating the bubble from the outside space (Fig. 7c). With laser-pulse termination, fast plume expansion results in a dramatic decrease of vapor pressure above the target surface that, in its turn, causes the vapor bubble to grow further and to burst eventually (Fig. 7d). Such a picture is most likely to develop for materials allowing considerable subsurface heating, as discussed above. Possibly, the described phenomenon is responsible for PLA craters with spallated surface slabs which can arise as a result of vapor ejection from the target depth, while the outer colder layers may be solidified in the irradiated spot edges [30].

An experimental study could in principle clarify whether the boiling crisis does occur due to subsurface heating on laser ablation. If so, it imposes a restriction on the application of our model at high fluences. On the other hand, formation of a vapor bubble beneath the surface should reduce the subsurface-heating effect due to latent heat of vaporization. On can speculate therefore that the T_c values evaluated in the present calculations (Table 3) provide the upper limits in estimations of the thermodynamic critical temperature. A more sophisticated model is needed to describe the thermal pro-

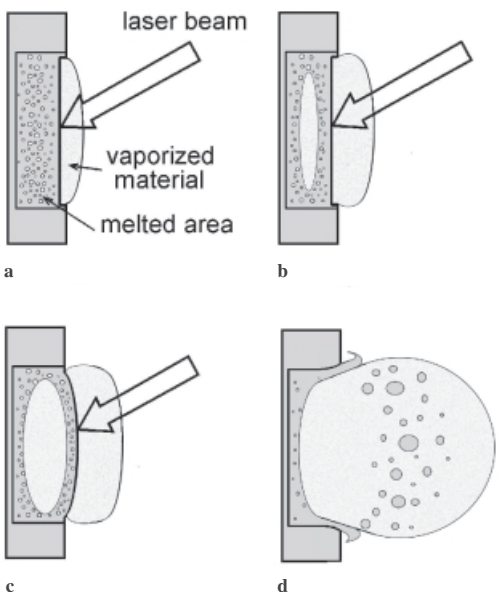

Fig. 7. Schematic representation of the development of a 'boiling crisis' during PLA of solids. Due to superheating of the subsurface layers of the target material, the vapor nuclei coalesce, resulting in a large bubble that bursts after laser-pulse termination

cesses in the target under the conditions when the boiling crisis develops.

3 Conclusions

The experimental evidence for the transition from normal vaporization to phase explosion during PLA of graphite, niobium and YBCO superconductor has been obtained and the corresponding values of threshold fluences have been determined. The thermal heating process in the irradiated targets has been characterized using model calculations. Further, based on the theory of the critical state of matter, the phase-explosion mechanism of laser ablation has been considered from the viewpoint of approaching the thermodynamic critical temperature. It is also our opinion that phase explosion is not the only manifestation of the critical phenomena during PLA. For example, a sort of 'boiling crisis' may be expected. The boiling crisis is likely to be an inherent feature for ns (and possibly ps) laser pulses and may exist in a range of laser fluences above which equilibrium thermodynamics can not be applied, so that a solid experiences a transition to the supercritical state. For fs laser pulses, ablation appears to start from such a transition [33]. Thus, the dominant mechanisms of laser ablation at ns time scales may be listed in order of increasing laser fluence as follows: normal vaporization, phase explosion with a possibility of boiling crisis for materials allowing for large subsurface heating and transition 'solid–supercritical matter'. Above the threshold of the transition to the supercritical state, a narrow range of laser fluence would be expected wherein a rarefaction shock wave reveals itself [34]. The fluence ranges of the listed mechanisms depend on substance properties and differ for different pulse durations.

It is conceivable that many obscure effects observed on laser ablation can be understood in terms of the thermodynamic critical state of matter. On the other hand, laser ablation has great potential as a means of investigating matter under critical and supercritical conditions. As an example, recent experimental evidence of rarefaction-wave formation under short laser-pulse ablation [35] opens new possibilities for the study of critical phenomena [34].

Acknowledgements. We thank Prof. E.E.B. Campbell and Dr. A.B. Kaplun for valuable discussions. This work was supported by the Russian Foundation for Basic Research (Grants 99-03-32331 and 99-03-33372) and by the Russian Scientific and Technical Program 'Fullerenes and Atomic Clusters' (Project 5-4-99). Financial support by the Royal Swedish Academy of Sciences Russian–Swedish exchange program is also gratefully acknowledged.

References

1. A. Miotello, R. Kelly: Appl. Phys. Lett. **67**, 3535 (1995)
2. R. Kelly, A. Miotello: Nucl. Instrum. Methods. B **122**, 374 (1997)
3. A. Miotello, R. Kelly: Appl. Phys. A **69**, S67 (1999)
4. M.M. Martynyuk: Russ. J. Phys. Chem. **57**, 494 (1983)
5. D.B. Geohegan: Appl. Phys. Lett. **62**, 1463 (1993)
6. K.H. Song, X. Xu: Appl. Surf. Sci. **127–129**, 111 (1998)
7. R. Kelly, A. Miotello, A. Mele, A. Giardani Guidoni, J.W. Hastie, P.K. Schenck, H. Okabe: Appl. Surf. Sci. **133**, 251 (1998)
8. J.H. Yoo, S.H. Jeong, X.L. Mao, R. Greif, R.E. Russo: Appl. Phys. Lett. **76**, 783 (2000)
9. L.V. Zhigilei, B.J. Garrison: Appl. Surf. Sci. **127–129**, 142 (1998)
10. R. Stoian, H. Varel, A. Rosenfeld, D. Ashkenasi, R. Kelly, E.E.B. Campbell: Appl. Surf. Sci. **165**, 44 (2000)
11. R. Kelly, A. Miotello: Appl. Surf. Sci. **96–98**, 205 (1996)
12. V.P. Skripov: *Metastable Liquids* (Halsted, New York 1974)
13. M.A. Anisimov: Sov. Phys. Usp. **17**, 722 (1975)
14. T. Götz, M. Bergt, W. Hoheisel, F. Träger, M. Stuke: Appl. Surf. Sci. **96–98**, 280 (1996)
15. A.V. Bulgakov, N.M. Bulgakova: Quantum Electron. **29**, 433 (1999)
16. A. Peterlongo, A. Miotello, R. Kelly: Phys. Rev. E **50**, 4716 (1994)
17. V.N. Tokarev, J.G. Lunney, W. Marine, M. Sentis: J. Appl. Phys. **78**, 1241 (1995)
18. S. Fähler, H.-U. Krebs: Appl. Surf. Sci. **96–98**, 61 (1996)
19. A. Giardini Guidoni, R. Kelly, A. Mele, A. Miotello: Plasma Sources Sci. Technol. **6**, 260 (1997)
20. Ya. Zeldovich, Yu.P. Raizer: *Physics of Shock Waves and High Temperature Hydrodynamic Phenomena* (Academic, New York 1996)
21. A.A. Samokhin, A.B. Uspensky: Sov. Phys. JETP **46**, 543 (1977)
22. A.A. Samokhin, A.B. Uspensky: Phys. Lett. A **73**, 391 (1979)
23. A.A. Samokhin: Trudy IOPAN **13**, 3 (1988) (in Russian)
24. S.I. Anisimov, A.M. Bonch-Bruevich, M.A. El'yashevich, Ya.A. Imas, N.A. Pavlenko, G.S. Romanov: Sov. Phys. – Tech. Phys. **11**, 935 (1967)
25. C.M. Guldberg: Z. Phys. Chem. **5**, 374 (1890)
26. R.C. Reid, T.K. Sherwood: *The Properties of Gases and Liquids* (McGraw-Hill, New York 1966)
27. I.B. Sladkov: Russ. J. Phys. Chem. **58**, 1250 (1984)
28. V.E. Fortov, A.N. Dremin, A.A. Leontyev: High Temp. **13**, 1072 (1975)
29. A.A. Likalter: Phys. Rev. B **53**, 4386 (1996)
30. C. Körner, R. Mayerhofer, M. Hartmann, H.W. Bergmann: Appl. Phys. A **63**, 123 (1996)
31. S.S. Kutateladze: *Fundamentals of Heat Transfer* (Academic, New York 1963)
32. R. Kelly, A. Miotello: Phys. Rev. E **60**, 2616 (1999)
33. B.N. Chichkov, C. Momma, S. Nolte, F. von Alvensleben, A. Tünnermann: Appl. Phys. A **63**, 109 (1996)
34. N.M. Bulgakova: Phys. Rev. E **60**, R3498 (1999)
35. K. Sokolowsky-Tinten, J. Bialkowsky, A. Cavalleri, D. von der Linde, A. Oparin, J. Meyer-ter-Vehn, S.I. Anisimov: Phys. Rev. Lett. **81**, 224 (1998)